

Local structural properties in nanocrystals CeAl_2 , CePt_2 and $\text{CePt}_{2.5}$

S.-W. Han,¹ C. H. Booth,² E. D. Bauer,³ P. H. Huang,⁴ Y. Y. Chen,⁴ and J. M. Lawrence⁵

¹*Chonbuk National University, Jeonju, 561-756, Korea*

²*Chemical Sciences Division, Lawrence Berkeley*

National Laboratory, Berkeley, California 94720, USA

³*Los Alamos National Laboratory, Los Alamos, New Mexico 87545, USA*

⁴*Institute of Physics, Academia Sinica, Taipei, Taiwan, Republic of China*

⁵*Department of Physics, University of California, Irvine, California 92697, USA*

(Dated: October 16, 2003)

Abstract

When antiferromagnetic CeAl_2 , CePt_2 and $\text{CePt}_{2.5}$ crystallites are reduced to nanometer scale particle sizes, their physical properties become that of a nonmagnetic Kondo system. Although particle size likely plays a dominant role, structural changes between the bulk and nanoscale particles may also play an important role. Since the small particle sizes limit the utility of diffraction experiments, the local structural properties of bulk and nanocrystalline CeAl_2 , CePt_2 and $\text{CePt}_{2.5}$ samples were studied by x-ray absorption fine structure measurements (XAFS) at the Ce and Pt L_3 -edges. In CeAl_2 , the XAFS studies show that the nanocrystalline material is severely disordered compared to its bulk counterpart and that the nearest-neighbor Ce-Al bond length is about 0.4 Å shorter in the nanocrystal than in the bulk. In CePt_2 and $\text{CePt}_{2.5}$, we also find that the local structure in the nanocrystals has a large amount of disorder/distortion from all atom sites and that the Ce atom is in a mixed valence state between Ce^{3+} and Ce^{4+} . These observations strongly suggest that in addition to size and surface effects, structural disorder plays a role in determining the Kondo behavior in these nanocrystals.

PACS numbers: 72.15.Qm, 61.10.Ht, 71.23.-k, 61.46.+w

I. INTRODUCTION

- 1) Describe the studies on CeAl_2 .
- 2) Describe the studies on CePt_{2+x} .

The antiferromagnetically ordering temperature in CePt_2 is known at $T_N \simeq 2 \text{ K}^{4-7}$. As the particle size is in a nanometer scale, the T_N moves toward to further low temperature³.

The effect of particle size on physical and electronic properties has attracted broad interest with many studies reported on this subject, both experimentally and theoretically². The CeAl_2 , CePt_2 and $\text{CePt}_{2.5}$ display the fascinating property that as its particle size becomes comparable to the nanometer scale, the system transitions from displaying magnetic order to Kondo behavior. This transition has been explained in terms of size and surface effects³. However, structural changes in the nanosize crystals may also be relevant. We explored this possibility through local structure measurements of bulk and nanocrystalline CeAl_2 , CePt_2 and $\text{CePt}_{2.5}$ using the x-ray absorption fine-structure technique (XAFS) which can detect both the bond length and the disorder of a near-neighbor atomic pair from a selected atom species. In addition, we can obtain the electronic properties of $4f$ -valence state from the x-ray absorption measurements at the Ce L_3 -edge.

For the XAFS measurements, the bulk samples CeAl_2 , CePt_2 and $\text{CePt}_{2.5}$ were fabricated by arc melting and the $\sim 80 \text{ \AA}$ diameter nanocrystals were obtained using a liquid-nitrogen cold trap³. The crystals were ground and sieved through a $25 \text{ }\mu\text{m}$ sieve. The sieved powder was uniformly spread over adhesive tape which was folded several times to obtain the absorption edge step of $0.3 - 1.0$. Transmission Ce and Pt L_3 -edge (5724 and 11564 eV , respectively) XAFS measurements from CeAl_2 and $\text{CePt}_{2.5}$ at $T = 20 \text{ K}$ were made at beamline 2-3 of the Stanford Synchrotron Radiation Laboratory (SSRL) and the measurements on CePt_2 were done at the PNC-CAT of the Advanced Photon Source (APS) using a $1/2$ (SSRL) and $1/4$ (APS)-tuned Si(111) double monochromator.

Figure 1 shows the normalized total x-ray absorption (μx) from CeAl_2 (a) and CePt_2 (b) at Ce L_3 -edge as a function of incident x-ray energy. The relatively sharper white line from the nano crystal indicates narrowing energy band due to the nano crystal size. More interesting feature is found in (b), which is measured on CePt_2 . There is an obvious peak existing in the nanocrystal data just after the absorption edge. We find the same feature

from the CePt_{2.5} nanocrystals. In the $2p$ - $5d$ electron transition under the mixed states of Ce³⁺ ($4f^15s^1$) and Ce⁴⁺ ($4f^05s^2$), the strange shape above the post-absorption edge has been studied by Sham *et al.*¹³ Our observation strongly suggests that the Ce atom has the mixed state of Ce³⁺ and Ce⁴⁺. We will discuss this with the structural properties later in detail.

The oscillation part in the post-edge has been well-known as the XAFS modulation which is directly related to the atomic local structure⁸. The XAFS was analyzed with the UWXAFS package⁹ (methods are described elsewhere¹⁰), using the photoelectron back scattering functions calculated with the FEFF8 code¹¹. After the atomic background was subtracted from the raw data using the AUTOBK which is a part of the UWXAFS package, the XAFS modulation (χ) was obtained. Figure 2 shows the XAFS from CeAl₂, CePt₂ and CePt_{2.5} nanocrystals and their bulk counterparts at Ce and Pt L_3 -edges. The weak intensity of the XAFS data indicates that the local structures in the nanocrystals are considerably disorder, comparing with those in their bulk counterparts. We analyzed the XAFS in r -space after the XAFS data from L_3 -edge within $2.7 - 7.5 \text{ \AA}^{-1}$ and $2.5 - 9.5 \text{ \AA}^{-1}$ for the nano and bulk specimens, respectively, were Fourier transformed. For the Fourier transform, the Hanning window with the window sills of 0.5^{-1} was used.

Figure 3 shows the magnitude of Fourier transformed XAFS data from bulk and nanocrystalline samples of CeAl₂. Note that the peaks are shifted on the \tilde{r} axis from their true bond lengths due to the phase shift of the back scattered photoelectron. Detailed fits are therefore necessary to obtain quantitative information. Fits to the bulk data start from the $C15$ Laves structure (space group ($fd\bar{3}m$)), allowing the bond length and the Debye-Waller factor (σ^2 , including thermal vibrations and static disorder) for each shell below 7 \AA to vary. The fitting paramers are summarized in Table I. We find that the Ce atoms have 12 Al neighbors at $3.356 \pm 0.005 \text{ \AA}$ and 4 Ce neighbors at $3.503 \pm 0.006 \text{ \AA}$. The σ^2 s are $0.0038 \pm 0.0004 \text{ \AA}^2$ for the Ce-Al pairs and $0.0021 \pm 0.0007 \text{ \AA}^2$ for the Ce-Ce pairs, respectively. These small σ^2 s suggest that the crystalline structure is well ordered. We derive a lattice constant of $8.095 \pm 0.015 \text{ \AA}$ from these data, roughly consistent with the previous x-ray diffraction measurement of 8.054 \AA ¹².

The nanoparticle fits also start from the bulk model, but reliable results are only obtained from shells shorter than 3.5 \AA . The inset shows the various fits assuming that only aluminum, only oxygen, or mixed Al and O occupy the Al site. The models using only Al or only O do not fit the measured data satisfactorily. The fit is considerably improved by including

about $10 \pm 5\%$ oxygen into the Al site. This observation of oxygen in the Al site agrees with the previous study³. In any case, these results strongly suggest that the Al site is partially occupied by oxygen. The best fit shows that the bond lengths are 2.44 ± 0.03 Å and 2.96 ± 0.02 Å for Ce-O and Ce-Al pairs, respectively. The σ^2 s in the nanoparticles are 0.044 ± 0.014 Å² for 11 ± 5 of aluminum neighbors and 0.005 ± 0.009 Å² for 1.3 ± 0.9 of oxygen neighbors. The average σ^2 of the Ce-Al and Ce-O pairs is about an order of magnitude larger than that of the Ce-Al pair in the bulk and the bond length of Ce-Al is about 0.4 Å shorter than the bond length of Ce-Al in the bulk. These measurements indicate that both large distortions and intrinsic disorder exist around Ce in the nanocrystals compared to the bulk.

In the analysis of the CePt₂ and CePt_{2.5} XAFS data, we have used the same method as mentioned above. In the CePt_{2.5}, the disordered C15 structure where the extra Pt randomly spreads onto all Ce sites⁴ was started. Figure 4 shows the amplitude of XAFS from CePt_{2.5} crystals at Ce *L*₃-edge (a) and Pt *L*₃-edge (b). The XAFS data shown in Fig. 2 within 2.7 – 8.0 and 2.7 – 9.5 Å⁻¹ for nano and bulk samples, respectively, were Fourier transformed. From the analysis on the bulk sample, we find the lattice constant of 7.71 ± 0.05 Å which agrees well with the study by Lawrence *et al.*⁴. With a fully occupied model, the analysis shows that 12 Pt and 4 Ce atoms are located at 3.175 ± 0.008 Å and 3.439 ± 0.007 Å, respectively. The σ^2 are 0.013 ± 0.001 and 0.003 ± 0.001 Å² for the Ce–Pt and Ce–Ce pairs, respectively. From this local structural studies, we find that the bond lengths of Ce–Pt is about 0.02 Å shorter while the Ce–Ce pairs has about 0.1 Å longer bond length than those in the crystalline symmetry. The fit parameters are summarized in Table II.

The XAFS data from the nanocrystals were also analyzed with assuming the same crystalline structure of the disordered C15 crystalline symmetry. The data in Fig. 4 (a) are the Fourier transformed amplitude of the data in Fig. 2 within the *k*-range of 2.7 – 8.0 Å⁻¹. A satisfactory fit can be obtained with a mix model of Ce and O for the nearest neighbor. The fit shows that $15 \pm 5\%$ of oxygen is occupied at the Pt site. The bond length of Ce–O and Ce–Pt pairs are 2.39 ± 0.02 and 2.843 ± 0.007 Å with σ^2 s of 0.021 ± 0.001 Å². Because of the high correlation of the σ^2 s between Ce–O and Ce–Pt pairs, a single σ^2 was used for the both pairs in the fit. In the consecutive neighbors, 4 Ce–Ce, 16 Ce–Pt and 12 Ce–Ce pairs have the bond lengths of 3.29(1), 4.46(2) and 5.03(2) Å with σ^2 of 0.024(2), 0.028(4) and 0.021(3) Å², respectively. The analysis shows that the bond lengths in the nanocrystals

are about 4–5 Å shorter than those in the bulk and the σ^2 s are about 1.5–2 times larger than those in the bulk counterpart.

Figure 4 (b) shows that the XAFS data from CePt_{2.5} at Pt L_3 -edge. Unlikely Ce L_3 -edge, we do not observe a special difference at the near edge which is not shown here. The data were Fourier transformed from the data in Fig. 2 within the k -range of 2.5 – 14.5 Å⁻¹ and 2.5 – 11.5 Å⁻¹ for the bulk and nano specimens, respectively. The analysis the data for the bulk was started with the crystalline symmetry mentioned above. The bond lengths and σ^2 s of the atomic pairs are summarized in Table II.

II. CONCLUSIONS

we have studied the local structural properties of nanocrystalline CeAl₂, comparing with its bulk counterpart. A substantial amount of disorder in the nanoparticle is observed and the Ce-Al bond length is shorter than that in the bulk. Moreover, oxygen is observed in the Al site. These changes in the structural properties should be included in any proper theory of the changes in the physical properties of nanocrystalline CeAl₂.

Acknowledgments

This work is supported in part by the Office of Science, U.S. Department of Energy (DOE) under Contract No. DE-AC03-76SF00098. Data were collected at the SSRL, a national user facility operated by Stanford University for the DOE, Office of Basic Energy Sciences.

¹

² W. P. Halperin, Rev. Mod. Phys. **58**, 533 (1986).

³ Y. Y. Chen, Y. D. Yao, C. R. Wang, W. H. Li, C. L. Chang, T. K. Lee, T. M. Hong, J. C. Ho, and S. F. Pan, Phys. Rev. Lett. **84**, 4990 (2000). The studies on CePt₂ will be published.

⁴ J. M. Lawrence, Y.-C. Chen, G. H. Kwei, Phys. Rev. B **56**, 5 (1997).

- ⁵ L. Rebelsky, K. Reilly, S. Horn, H. Borges, J. D. Thompson, R. Caspary, J. Appl. Phys. **67**, 5206 (1990).
- ⁶ R. R. Joseph, K. A. Gschneidner, Jr., R. E. Hungsgerg, Phys. Rev. B **5**, 1878 (1972).
- ⁷ A. B. Andrews, J. J. Joyce, A. J. Arko, J. D. Thompson, J. Tang, J. M. Lawrence, J. C. Hemminger, Phys. Rev. B **51**, 3277 (1995).
- ⁸ E. A. Stern, Phys. Rev. B **10**, 3027 (1974); J. J. Rehr, R. C. Albers, S. I. Zabinsky, Phys. Rev. Lett. **69**, 3397 (1992).
- ⁹ E. A. Stern, M. Newville, B. Ravel, Y. Yacoby and D. Haskel, Physica B **208 & 209**, (1995) 117; Find further information of UWXAFS at <http://depts.washington.edu/uwxafs>.
- ¹⁰ S.-W. Han, E. A. Stern, D. Hankel, A. R. Moodenbaugh, Phys. Rev. B. **66**, (2002) 094101.
- ¹¹ A. L. Ankudinov, B. Ravel, J. J. Rehr, S. D. Conradson, Phys. Rev. B **58**, 7565 (1998).
- ¹² M. Croft and H. H. Levine, Phys. Rev. B **22**, 4366 (1980).
- ¹³ T. K. Sham, Phys. Rev. B **40**, 6045 (1989).

TABLE I: Results of least-squares fit at Ce L_3 -edge from CeAl₂ at 20 K. The total number of data points in the Fourier transformed XAFS is determined by Stern's rule⁹; $(2\Delta k\Delta r / \pi + 2)$ where Δk is the region of k in which the data were used for Fourier transform into r -space and Δr is the fit region.

Sample	χ^2_ν	r-factor	N_I	ν	S^2_0
Nano	12.4	0.0067	9	4	0.98 ± 0.10
Bulk	240.5	0.0105	29	16	0.90 ± 0.06

TABLE II: Bond lengths and σ^2 s in CePt₂ and CePt_{2.5} determined at Ce and Pt L_3 -edges at 20 K

Specimen	Ce L_3 -edge				Pt L_3 -edge			
	Ce–Pt		Ce–Ce		Pt–Pt		Pt–Ce	
	r(Å)	σ^2 (Å ²)	r(Å)	σ^2 (Å ²)	r(Å)	σ^2 (Å ²)	r(Å)	σ^2 (Å ²)
CePt ₂ (bulk)	3.18(1)	0.012(1)	3.43(1)	0.012(1)	2.723(1)	0.0015(1)	3.19(1)	0.013(1)
CePt ₂ (nano)	2.91(1)	0.018(2)	3.37(1)	0.025(2)	2.690(5)	0.0051(2)	2.86(5)	0.050(8)
CePt _{2.5} (bulk)	3.17(1)	0.014(1)	3.44(2)	0.0030(9)	2.714(1)	0.0019(1)	3.11(1)	0.014(1)
CePt _{2.5} (nano)	2.84(1)	0.021(1)	3.29(1)	0.026(2)	2.690(3)	0.0054(3)	2.99(7)	0.038(9)

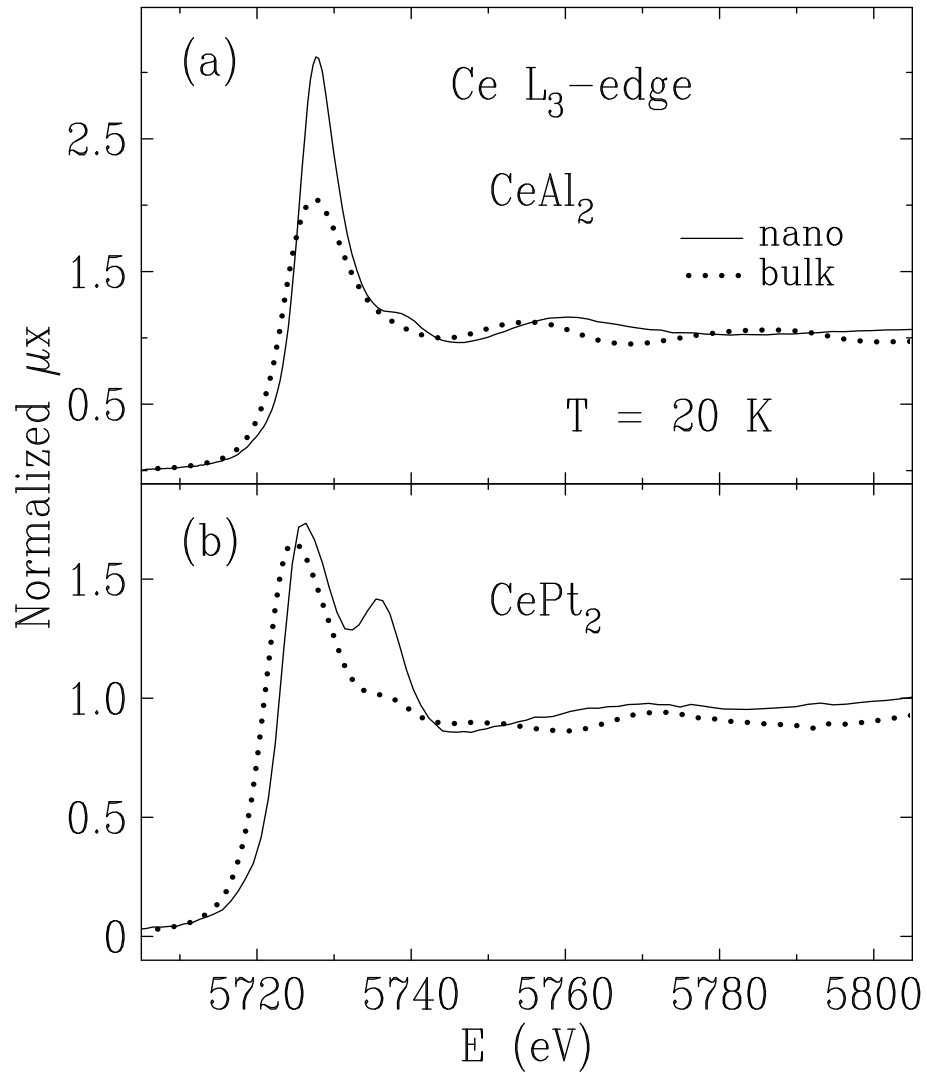


FIG. 1: Normalized total X-ray absorption as a function of incident x-ray energy at Ce L_3 -edge on CeAl_2 (a) and CePt_2 (b).

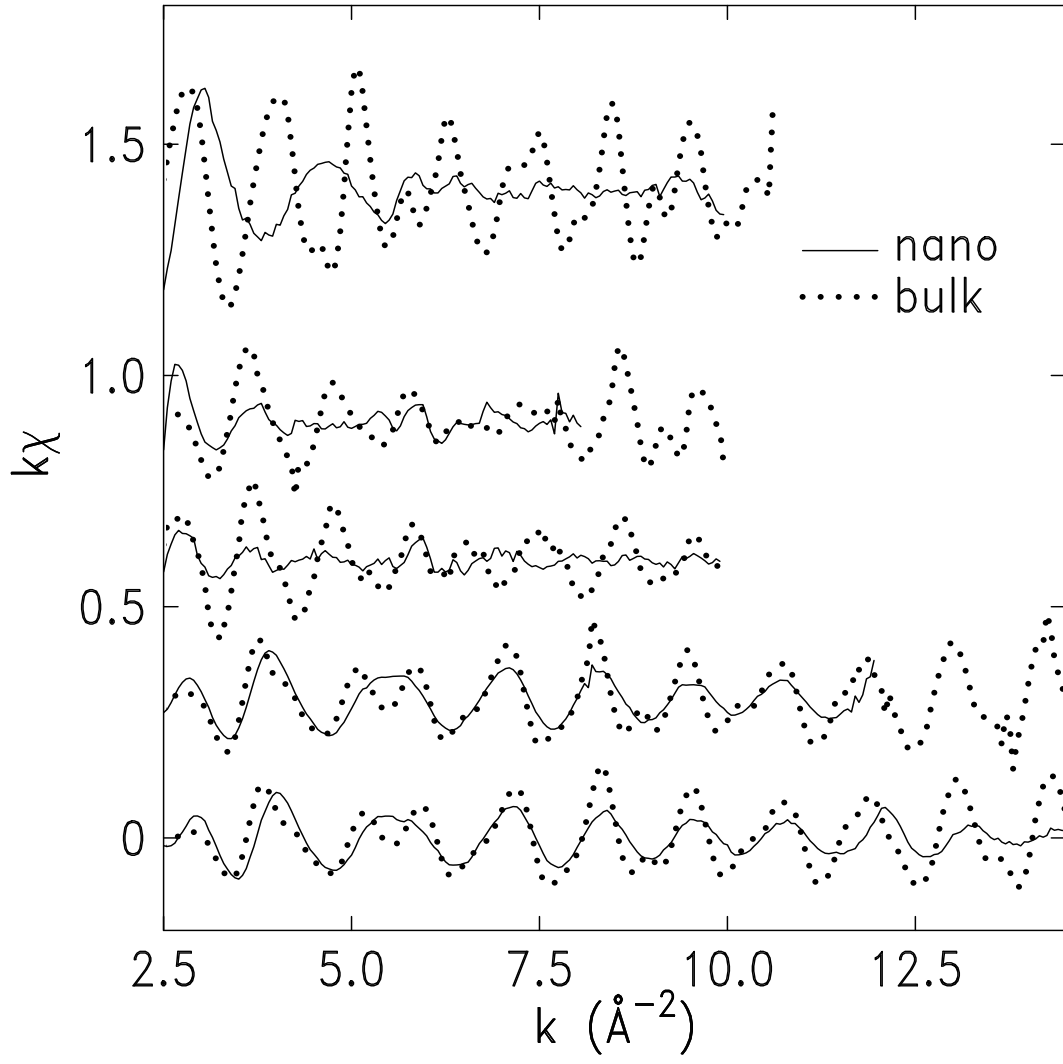


FIG. 2: XAFS ($k\chi$) as a function of wave number vector k measured at 20 K. From top, Ce L_3 -edge on CeAl_2 , CePt_2 and $\text{CePt}_{2.5}$, and Pt L_3 -edge on CePt_2 and $\text{CePt}_{2.5}$. The XAFS data could not be obtained beyond $k = 10 \text{ \AA}^{-1}$ at Ce L_3 -edge due to the Ce L_2 -edge.

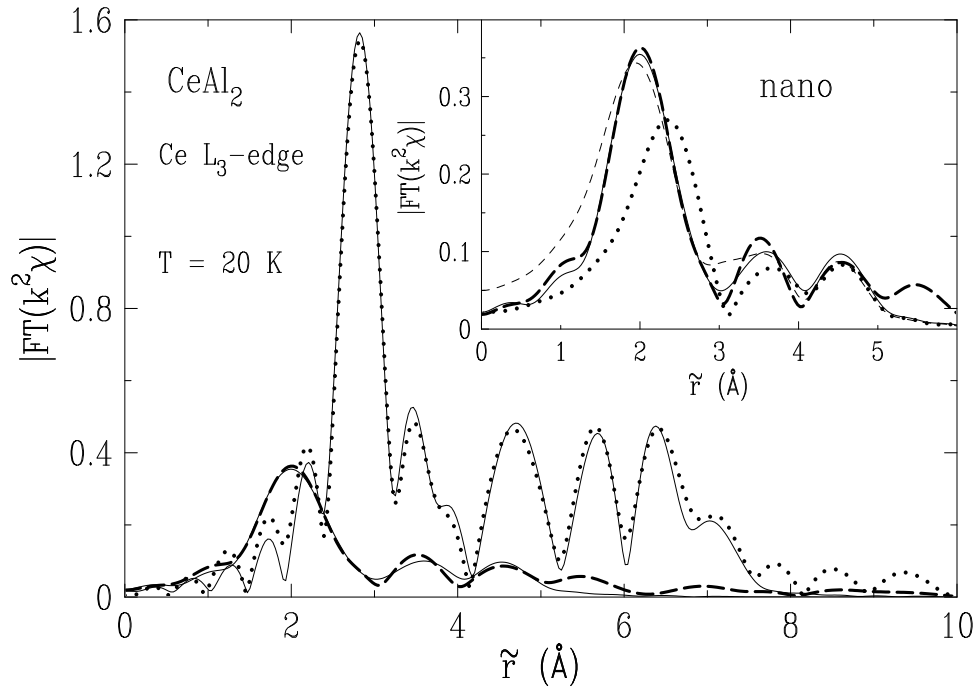


FIG. 3: Magnitude of Fourier transformed XAFS data from a bulk (dotted line) and a nanocrystal (thick-dashed line) of CeAl_2 as a function of distance from probe atom Ce. Solid lines are best fits. Inset indicates the XAFS data from the nanoparticle CeAl_2 and fits with the different models of Al-O mixed (solid line), Al only (dotted line) and O only (thin-dashed line).

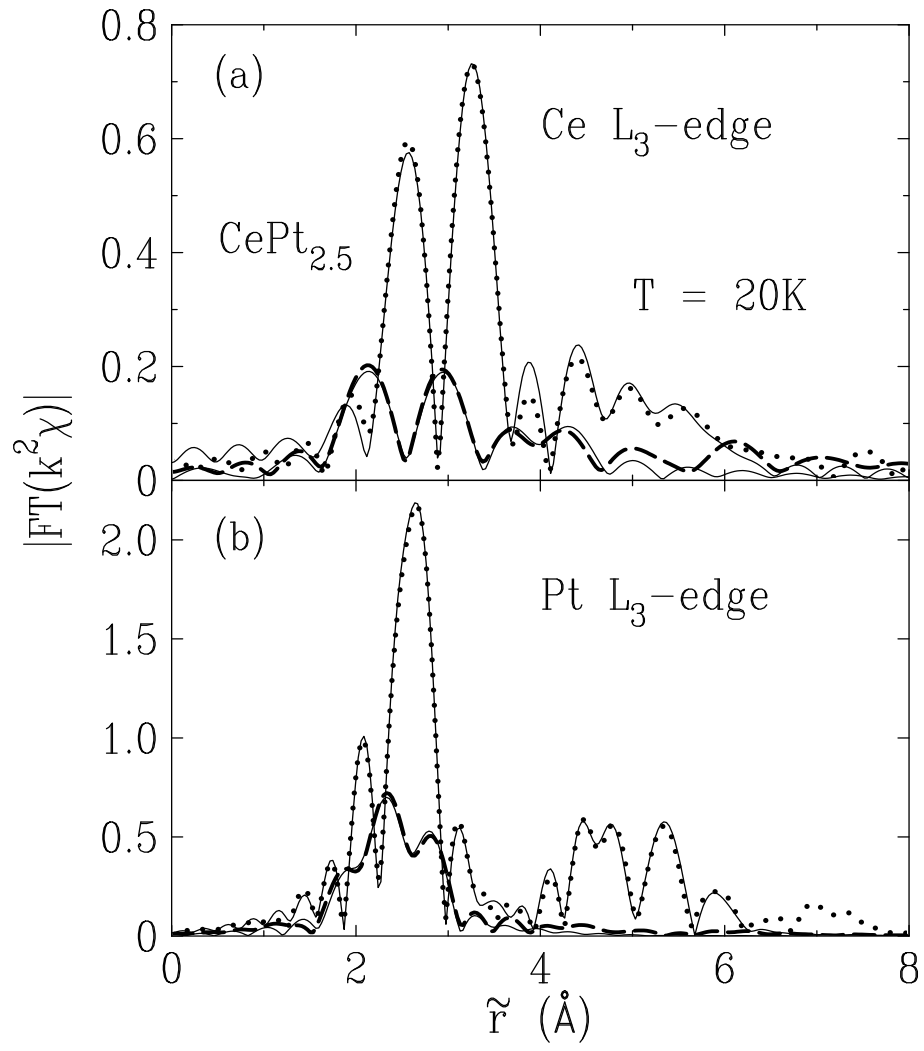


FIG. 4: Magnitude of Fourier transformed XAFS data from a bulk (dotted line) and a nanocrystal (thick-dashed line) of CePt_{2.5} as a function of distance from probe atom Ce (a) and Pt (b). Solid lines are best fits.

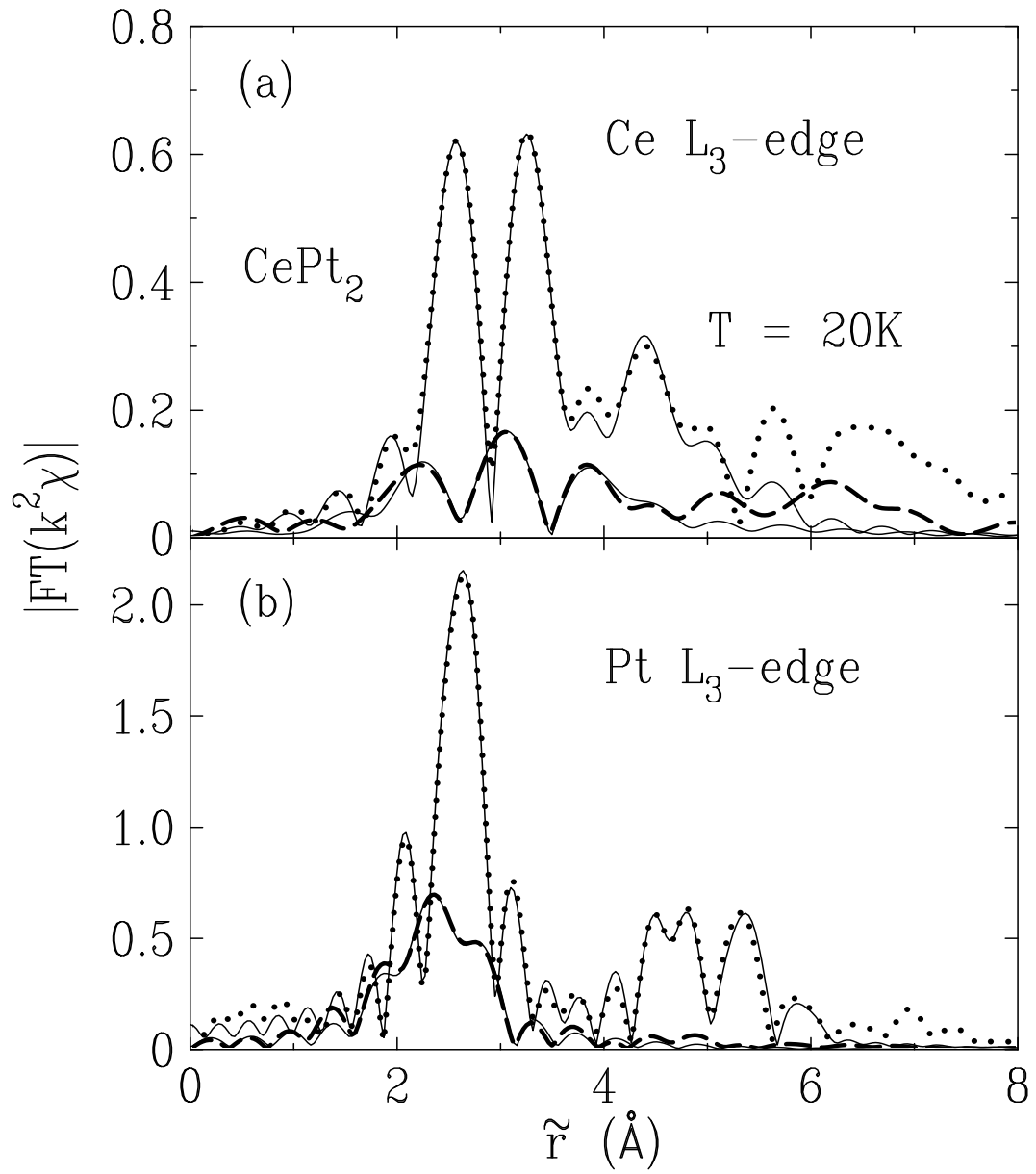


FIG. 5: Magnitude of Fourier transformed XAFS data from a bulk (dotted line) and a nanocrystal (thick-dashed line) of CePt₂ as a function of distance from probe atom Ce (a) and Pt (b). Solid lines are best fits.